Ionic distribution around simple DNA models. I. Cylindrically averaged properties

J. C. Gil Montoro and J. L. F. Abascal
Departamento de Química-Física, Facultad de Ciencias Químicas, Universidad Complutense de Madrid, E-28040 Madrid, Spain

(Received 8 February 1995; accepted 8 August 1995)

Properties depending on the radial ionic concentration profiles are calculated by Monte Carlo simulation for several simple B-DNA models in the presence of added (monovalent) salt up to 2.5 M concentration. The models include both homogeneously and discretely charged polyions. Besides, the effect of hard and soft repulsive forces is considered. A novel model which represents the DNA grooved structure in a simplified manner is introduced. From a methodological point of view, special attention is paid to the treatment of long-range forces along the axial direction. Exact formulas for discretely charged polyelectrolytes are used. Regarding the density profile results, it is concluded that the main effect is not due to the discreteness of the positions of the charges, i.e., homogeneously charged models lead to properties not significantly different from discretely charged ones. A similar statement holds for the comparison between hard and soft models. Nevertheless, the inclusion of the grooved shape of DNA modifies this behavior. A double hump in the concentration profile function is brought about by the coupling between repulsive and coulombic forces in the grooved model. It is shown that not only this but also other properties of full atomic models of DNA are adequately predicted by our simplified grooved model. Finally, at high concentrations of added salt, it is seen that the condensed ionic cloud overneutralizes the polyelectrolyte charge. This charge reversal phenomenon, which is observed in all the models studied, has not been previously observed due to the high salt concentration required. © *1995 American Institute of Physics.*

I. INTRODUCTION

Added to its singular biological role as the carrier of the genetic information, DNA in solution exhibits typical polyelectrolyte properties such as strong thermodynamic nonideality of counterions which—contrary to the behavior in simple electrolyte solutions[1]—*increase* with dilution. The reason is the high density charge created by the complete ionization of the acidic phosphate groups[2] which, together with the DNA periodicity and its local helical symmetry, induces long-range Coulomb interaction with the surrounding charged entities such as ions, proteins, or other nucleic acids. Experimental properties that depend essentially on the mean electrostatic field far from the polyion (osmotic pressure, activity coefficients, or Donnan equilibria)[3] have been explained in terms of very crude DNA models like the line of charge of the counterion condensation (CC) theory of Manning,[4–7] or the Poisson–Boltzmann (PB) theory applied to the homogeneously charged cylinder.[8–10] (A comparison between the CC and PB methods can be found in Ref. 11.) The latter model has been thoroughly investigated by Monte Carlo computer simulation.[10,12–15]

The detailed structure of DNA, on the other hand, is of increasing significance as one approaches its surface. This must be even more important for properties in which the polyion potential enters directly, such as NMR spectroscopy, diffusion, or conductivity.[16] For example, $^{23}Na^{+}$ splitting quadrupole coupling constants are significantly higher for a model in which discrete charges are placed in the surface of a cylinder than for the homogeneously charged model.[17] For this sort of property, as well as for the specific interaction of molecules with DNA, an all-atom model with explicit water and ions seems to be the natural choice (for a review on full-atom DNA molecular dynamics simulations see Ref. 18). Unfortunately, this approach suffers from various inconveniences. The huge computational demand of the simulations with explicit water coerces its application to small systems with few counterions, no added salt, and relatively short elapsed times (typically 80 ps,[19] although up to a nanosecond has been explored).[20] Other handicaps are convergence problems and strong dependence of the results on the initial conditions as a result of the high particle density combined with the system inhomogeneity[19,21] and the need for using debatable combination rules for the water–ion and water–DNA interactions.[22] The impossibility of including a consistent axial long-range potential within the usual mean field scheme in systems with explicit water has been also pointed out.[23] For these reasons, in the context of biophysical studies like drug–DNA or protein–DNA binding, few simulation studies have been conducted at the explicit water level of detail.[24] From a physicochemical point of view there is another major shortcoming in using such detailed models. The interplay between the different forces acting on each particle makes very difficult the assessment of the importance of each interaction. It is then very difficult to ascribe a given effect to a particular interaction. Moreover, the subtle competition between them makes it possible that similar simulation studies will lead to contradictory results.[21]

In this paper we have adopted a simple model approach since this allows us to learn the physics that a given refinement adds with respect to a previous level, thus unambiguously assigning each effect to its cause. In particular, we deal only with solvent continuum models (the McMillan–Mayer level) which offer a suitable alternative both for the under-

Downloaded 27 May 2005 to 147.96.5.17. Redistribution subject to AIP license or copyright, see http://jcp.aip.org/jcp/copyright.jsp

standing of the ionic atmosphere around DNA[25] and for molecule–DNA interactions.[19] Getting rid of explicit water molecules enables the extension of the range of applicability of the simulations, going beyond the salt-free case or doing larger runs. Additionally, Grand Canonical ensemble simulations become feasible. Although effects due to the microscopic heterogeneity of water such as hydration, solvation, and hydrogen bonding are missing, some of them may be accommodated back into the model (for example, the hydration sphere is usually accounted for through an increase in the ionic effective radius).

In the treatment of solutions at the McMillan–Mayer level, the water effects are introduced as a modification of the electrostatic interaction between charges by means of a dielectric function. But the dielectric effects induced by the polyelectrolyte are rather complex. There is a lowering of the dielectric properties of the first layers of solvent molecules as a result of their polarization in the strong electric field (the dielectric saturation effect). Besides, image forces appear due to the polarization of the interface between the macromolecule and the surrounding ions (the dielectric discontinuity effect).[26] The latter effect has been estimated by Troll *et al.*[27] by direct measurements of a macroscopic model in an electrolyte tank. Although their analysis is expected to give the trends for this complex effect, the actual quantitative results should be taken with some caution. First, the tank walls preclude field lines from escaping so that the estimates correspond to zero boundary conditions in the finite difference Poisson–Boltzmann terminology.[28] Furthermore, Tanford and Kirwood, in their application of Kirwood's discrete charge model of proteins to titration curve calculations, found that almost any potential could be obtained when the depth of the discrete charge below the surface was varied.[26] It follows that the position of the DNA electrode in Troll *et al.* measurements may be critical. As a matter of fact, their measurements show a decrease of the grooves counterion population[27,29] with respect to what occurs in the unmodified model. The same effect considered through the finite difference Poisson–Boltzmann method shows the opposite trend,[28,30] at least up to physiological concentrations.

The dielectric saturation effect is usually modeled using a distance dependent dielectric constant.[31] With this modification to the Coulombic interaction, Jayaram *et al.* obtained significantly more condensed ions near DNA than with the unmodified potential.[21] Nevertheless, the water reorientational anisotropy in the vicinity of real polyelectrolytes similar to DNA (and hence the dielectric saturation) is minimal, as demonstrated by the NMR experiments of Halle and Piculell[32] (further interpreted by Leyte).[33] As a whole, the dielectric saturation and dielectric discontinuity effects are rather modest for hydrated univalent ions.[29] Moreover, the influence of both effects in several properties such as the energy or number of condensed counterions is the opposite,[21] and almost cancel each other. For all these reasons, we have chosen the basic option of approximating the dielectric function as a constant equal to the macroscopic dielectric permittivity of the bulk solvent, i.e., we deal with several models within the so-called ''primitive model.''

In this work we report Monte Carlo simulations of B-DNA in solution using several polyelectrolyte models at the continuum solvent level and a wide range of monovalent salt concentration. Our interest is to see the effects that DNA models of increasing detail have on the radial ionic atmosphere around it (for simplicity, we use either the terms radial or cylindrically averaged to refer to a property which is averaged over the cylindrical axial and angular coordinates so it only depends on the radial coordinate). Specifically, we compare structural features associated to homogeneous and discrete charge distribution. Both hard and soft repulsive potentials are used in this study although we focus our attention preferably on the more realistic soft case. A new simple model incorporating the grooved structure of DNA is introduced. In Sec. II we describe the different DNA models while Sec. III addresses methodological details of the simulations. The results and its discussion are presented in Sec. IV. The main conclusions are summarized at the end of the paper.

II. MODELS

Five models of B-DNA are compared in this work. In several models the polyion charge is homogeneously distributed while in others the charges are discretely placed at certain positions coincident with those of the phosphorus atoms in crystalline DNA. The discrete model is further improved by incorporating the grooved structure of DNA. The introduction and study of the latter model is in fact one of the main contributions of this work.

A. Homogeneously charged models

Our simplest model is the well-known homogeneously charged hard (HH) cylinder[8,9,34] (a summarized description of the models along with their acronyms is compiled in Table I). From the electrostatic point of view it is equivalent to a line of charge at the DNA axis but it is supplemented with a repulsive interaction to account for the DNA volume. The Coulombic interaction between an ion and the finite segment of the line of charge within the simulation box (of height L) is[10]

$$U_{\mathrm{ip}}^{\mathrm{line},L}(\rho_{\mathrm{ip}}) = -2z_i\xi\beta^{-1}\,\sinh^{-1}\left(\frac{L}{2\rho_{\mathrm{ip}}}\right), \tag{2.1}$$

where the subscript ip denotes a variable dependent on ion–polyelectrolyte distances. Accordingly, ρ_{ip} is the radial coordinate (distance to the polyelectrolyte axis) of ion i. Besides, z_i is the ionic electrovalence and ξ the reduced axial charge density of the polyion

$$\xi = \lambda_B / b, \tag{2.2}$$

b being the distance between charges along the polyelectrolyte axis ($b=1.69$ Å for B-DNA giving $\xi=4.23$) and λ_B the Bjerrum length. This is defined as

$$\lambda_B = \frac{e^2\beta}{4\pi\epsilon_0\epsilon}, \tag{2.3}$$

where e is the magnitude of the electronic charge, $\beta=1/(k_BT)$—k_B being the Boltzmann constant and T the temperature, ϵ_0 is the vacuum permittivity, and ϵ the (rela-

Downloaded 27 May 2005 to 147.96.5.17. Redistribution subject to AIP license or copyright, see http://jcp.aip.org/jcp/copyright.jsp

TABLE I. The simulations

DNA model	Nominal concentration (M)	Radial boundary	Number of ions[a]	Radial dimension (Å)[b]	Bulk concentration (M)[c]
Homogeneously charged hard cylinder (HH)	0.01	Cell	60+100	228.5	0.0107
	0.05	Cell	60+120	118.3	0.0483
	1	Cell	30+500	76.5	0.911
Homogeneously charged soft cylinder, origin[d] in axis (HS)	0.05	Cell	60+120	118.3	0.0487
	0.25	MBFB[e]	40+140	53.0	0.269
	1	MBFB	30+300	45.0	0.946
Homogeneously charged soft cylinder, origin displaced from axis (HS1)	0.05	Cell	60+120	118.3	0.0486
	0.1	Cell	60+120	81.3	0.106
	2.5	MBFB	30+240	28.0	2.484
Discretely charged soft cylinder, origin displaced from axis (DS)	0.05	Cell	60+120	118.3	0.0487
	1	MBFB	40+310	36.0	0.949
	2.5	MBFB	40+320	28.0	2.488
Grooved primitive model (GP)	Salt-free[f]	Cell	80+0	45.8	···
	0.05	Cell	60+120	118.3	0.0486
	0.1	Cell	60+120	80.8	0.106
	0.25	MBFB	40+130	50.0	0.270
	1	MBFB	40+205	32.5	0.989
	2.5	MBFB	20+194	22.0	2.490

[a]Compensating DNA charge counterions+added salt ion pairs.
[b]Cell radius in the cell model simulations and internal region radius in the MBFB simulations.
[c]Estimated uncertainties affect the last figure.
[d]It refers to the origin of the repulsive potential.
[e]Modulated bulk as a fuzzy boundary; see Ref. 36.
[f]Phosphate concentration 0.15 M.

tive) dielectric constant of the solvent. For water at 25 °C, $\epsilon=78.358$ and, thus, $\lambda_B=7.15$ Å. The repulsive part of the potential in this HH model is a hard-core one, i.e.,

$$U_{\mathrm{ip}}^{\mathrm{rep,hard}}(\rho_{\mathrm{ip}})=\begin{cases}\infty & \text{if } \rho_{\mathrm{ip}}<a\\ 0 & \text{otherwise}\end{cases}, \tag{2.4}$$

where the distance of closest approach a is the sum of the cylinder and ion radii. Although the traditional value for this parameter is 10+2=12 Å, the distance from the center of an hydrated Na ion to the B-DNA helix axis in the phosphate region, we reduce it to 8+2=10 Å to mimic the penetration of counterions within the DNA grooves. We will return to this point later.

A more realistic representation of the repulsive forces between ions and the polyion can be achieved through a soft potential. In fact, a soft repulsive polyelectrolyte model is able to explain the experimental results on the effect of DNA on rates of bimolecular energy transfer between ions in a more satisfactory way than a hard cylinder does.[35] The homogeneously charged-soft repulsive model (HS) keeps the homogeneous charge distribution of the previous model but replaces the hard-core repulsion by a soft potential of the form[12]

$$U_{\mathrm{ip}}^{\mathrm{rep,soft}}(\rho_{\mathrm{ip}})=K_{\mathrm{ip}}\frac{1}{\rho_{\mathrm{ip}}^{n}}. \tag{2.5}$$

With the steepness parameter taken as $n=9$, a value of $K_{\mathrm{ip}}=2.3466\times10^{-13}$ J Å^9 leads to a maximum in the radial distribution of counterions at about 11 Å.[36] (The parameter K_P in Ref. 36 is incorrect; it should read 6.0412×10^{-12} Jm/c.)

In the simulations with soft DNA, the mobile ions are considered to be soft as well. Thus,

$$U_{ij}^{\mathrm{rep}}(r_{ij})=K_{ij}\frac{1}{r_{ij}^{n}}, \tag{2.6a}$$

$$K_{ij}=\frac{A_M|z_iz_j|e^2}{4\pi\epsilon_0N_cn}(r_i+r_j)^{(n-1)}, \tag{2.6b}$$

r_{ij} being the distance between ions i and j. The choice of $A_M=1.7476$ (the Madelung's constant of the NaCl solid structure), and $N_c=6$ (the coordination number of the same structure) together with the value $r_i=1.4214$ Å (the nominal radius of ion i) taken for both anions and cations, gives bulk electrolyte properties approximately corresponding to a restricted primitive model with hard-sphere diameters of 4.2 Å.[37] This size has been widely used in recent electrolyte solution studies[14,38–42] and roughly corresponds to a sodium ion on account of its hydration shell.[39,43] Consistently, the hard sphere diameter of the ions in the simulations with the HH model is 4.2 Å.

B. Discretely charged models

A more significant refinement of the previous models is the substitution of the homogeneous charge by a (fixed) set of discrete charges. Most of the DNA charge lies at the phosphate groups.[2] Thus, as a reasonable approximation, we

Downloaded¬27¬May¬2005¬to¬147.96.5.17.¬Redistribution¬subject¬to¬AIP¬license¬or¬copyright,¬see¬http://jcp.aip.org/jcp/copyright.jsp

place unity negative charges at the phosphorus positions whose cylindrical coordinates for canonical B-DNA are[44]

$$\rho_i^s = 8.91,$$
$$\phi_i^s = \phi_0^s + 36i,$$
$$z_i^s = z_0^s + 3.38i, \tag{2.7}$$

where $s=1,2$ specifies the nucleic acid strand, $i=0,...,9$ describes a full DNA helix turn, ρ and z are given in angstrom, and ϕ in degrees. Besides, ϕ_0^s and z_0^s are both zero for the phosphates in the first strand, and 154.4° and 0.78 Å, respectively, for those in the second one. The 3.38 Å rise per residue and the 36° rotation lead to the well-known fact that B-DNA has ten base pair per helix turn with a 33.8 Å pitch. The potential between the charged DNA sites within the simulation box of height L and a mobile ion is simply

$$U_{\rm ip}^{{\rm sites},L} = \sum_\alpha U_{i\alpha}^{\rm cou}(r_{i\alpha}), \tag{2.8}$$

where the sum extends over DNA sites α, $r_{i\alpha}$ is the distance between site α and ion i, and $U_{i\alpha}^{\rm cou}$ is the coulombic potential energy which is obviously the same as the potential between any two (fixed or mobile) ions i,j

$$U_{ij}^{\rm cou} = \frac{z_i z_j}{4\pi\epsilon_0\epsilon}\frac{e^2}{r_{ij}}. \tag{2.9}$$

If the coulombic interaction were added to the repulsive potential of Eq. (2.5), an inconsistency would appear. The problem arises as counterions would (closely) approach a charged site. In such a case, its (arbitrarily large) attractive potential energy is not balanced by the repulsion of the soft cylinder which has its origin in the DNA axis, about 9 Å. With respect to the DNA charged site, the mobile ion behaves as a point-like charge, and collapses into it. In most simulations of discretely charged structures the problem does not arise due to the use of hard potentials.[13] Gordon and Goldman[23] simulated a Lennard-Jones- (LJ) type soft polyion core with discrete charges spiraling around it. They immersed the charges within LJ spheres to avoid this problem. The resulting model presented a bumpy surface due to the protruding spheres. Instead, we have modified the repulsive potential so that its origin coincides with the charged DNA sites,

$$U_{\rm ip}^{\rm rep,displaced}(\rho_{\rm ip}) = K'_{\rm ip}\frac{1}{(\rho_{\rm ip}-\rho_0)^n}. \tag{2.10}$$

For $n=9$ and $K'_{\rm ip} = 2.7291\times10^{-17}$ J Å^9—equivalent to an effective hard radius of 0.99 Å from the origin of the soft repulsion $\rho_0=8.91$ Å—the maximum in the radial distribution of counterions appears about $8.91+0.99+2.1=12$ Å, the usual closest approach distance in hard rod simulations. We refer to this model as DS (discretely charged, soft potential). For completeness, a few simulations have been done with the corresponding homogeneously charged soft potential (displaced from axis) model which will be referred to as HS1.

C. Grooved model

The last model in the series is devised to incorporate the accessibility of the DNA grooves to the small ions in a computationally tractable way. The idea lying behind the model is that the inhomogenizing effect of the helical arrangement of the negatively charged groups can be substantially enhanced by the excluded volume effects in the inner part of DNA making more apparent the inhomogeneity of the system along the axial direction. It is thus expected that counter- and coions can be accommodated in a different manner than in previous models. A few simulations considering the DNA grooves while treating water at the continuum level have been reported.[21,25,29,45] All but the first study (Ref. 29) dealt with *atomic DNA* (with the exception of hydrogens in some cases). It is our belief that, if water molecules are not present, this level of detail in the representation of DNA is not necessary. Since only the grooves' *shape* is relevant, it can be accounted for through a simplification of the DNA structure which in turn enables us to investigate without significant cost the effect of added salt at different concentrations. This enables new investigations as the previous studies treated the salt-free case (except in the last work where up to 0.1 M added salt was considered; nevertheless, structural results were not reported).

Troll *et al.*,[27] in their electrolytic tank study of modifications to the Coulombic potential near DNA, modeled from clay a solid with a kidney-shaped section and helical symmetry. This section was obtained as an envelope to the helical projection of the van der Waals surface of atomic DNA, and was subsequently employed in salt-free simulations.[29] From our point of view, an important objection to the model is that its surface is nonparametric which is uncomfortable for simulations (in Ref. 29 the simulations were done by mapping the surface onto a lattice). Moreover, the addition of a soft repulsive potential to this model would be a complicated task. We have proceeded in a similar way but the resulting surface has been roughly fitted to a set of geometrically simple objects. A cylinder mimics the central core of DNA, totally inaccessible to the mobile ions (corresponding to the paired purine and pirimidine bases). Two additional spheres complete each nucleotide. One (the phosphate sphere) centered at the position of the charges of Eq. (2.7) at a radial coordinate of 8.91 Å, and another one (the intermediate sphere) between the phosphate and the cylinder, at $\rho=5.90$ Å. The ϕ and z coordinates of both spheres are the same. We have further imposed that the repulsive interaction between these spheres and an ion have the same potential parameters as those between two mobile ions, i.e., the potential of Eq. (2.6) with $|z_i z_j|=1$. The charge distribution is the simple discrete distribution described above (unity charges placed at the phosphate positions). The phosphates are then both the charge carriers and the origin of repulsive interactions which is very convenient for the simulations. The internal repulsive cylinder is of the form of Eq. (2.10) with $\rho_0=2.91$ Å and the same $K'_{\rm ip}$ as the DS model.

The cylinder and the two spheres "overlap," the DNA major and minor grooves corresponding to the free areas between two opposite pairs of spheres. (A similar model has recently been employed by Rey and Skolnick[46] in the context of protein folding; there, each aminoacid was represented by two spheres, one corresponding to the backbone atoms and the other to the side chain). These parameters result in

Downloaded¬27¬May¬2005¬to¬147.96.5.17.¬Redistribution¬subject¬to¬AIP¬license¬or¬copyright,¬see¬http://jcp.aip.org/jcp/copyright.jsp

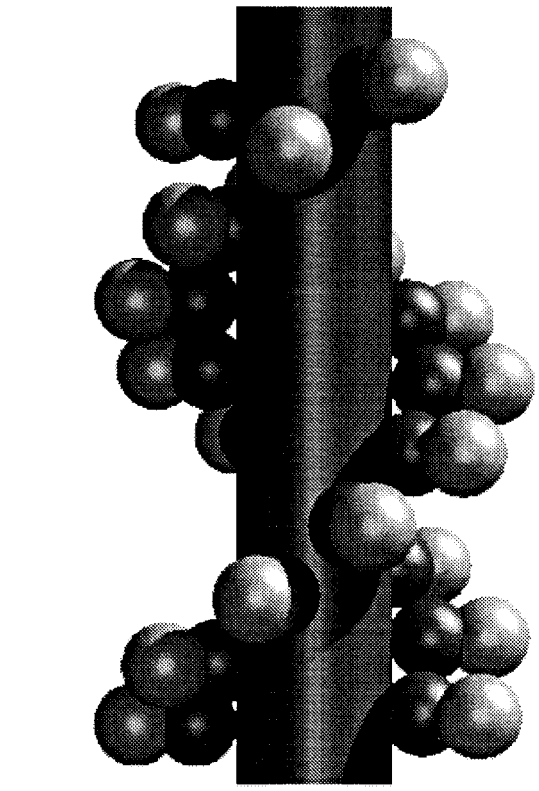

(a)

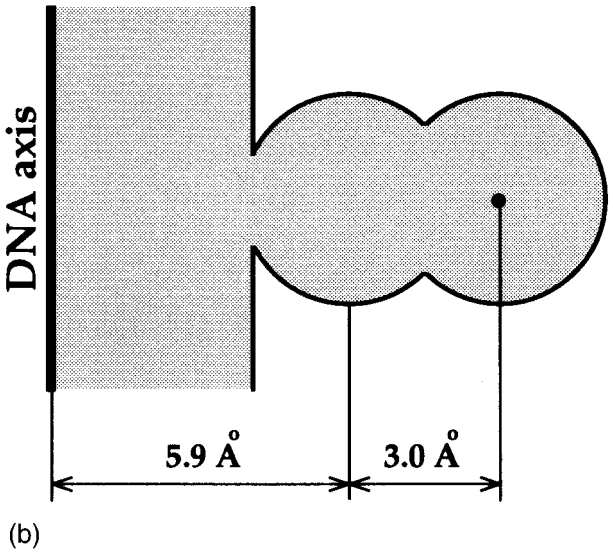

(b)

FIG. 1. (a) Space filling view of the grooved primitive model. (b) Half-section of the model showing the positions of the inner cylinder and the intermediate and phosphate spheres.

groove depth consistent with that of the Troll model (between 3.5 and 4 Å).[29] The ridge between the grooves appears continuous in real DNA while it looks discontinuous in our model because the space between the phosphates is empty. Nevertheless, there is not enough room between adjacent phosphates to accommodate an ion and, thus, the ridge appears continuous to the ions. The model will be referred to as GP (grooved primitive). To provide a visual idea, its essential features are shown in Fig. 1. Although the GP model is a soft

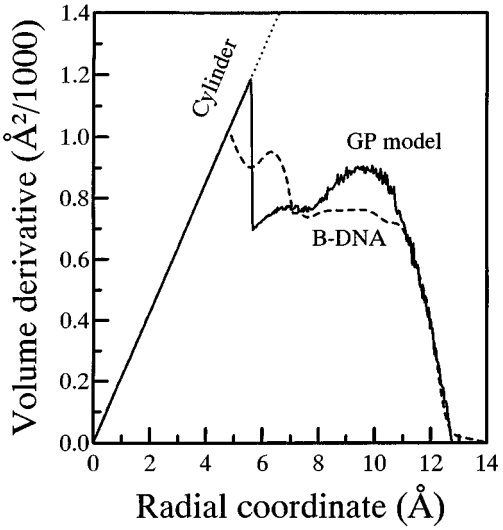

FIG. 2. Accessible and inaccessible volumes to mobile ions for canonical B-DNA (dashed line) and the grooved primitive model (solid line). The inaccessible volume at a given distance is the area below the corresponding curve, and the accessible one that between the curve and the straight dotted line. The DNA curve has been taken from Fig. 2 of Ref. 48.

one, we have been forced to depict it by means of a set of roughly equivalent hard bodies. This is done by defining the hard cores equal to the distance at the minimum of the soft potential (2.1 Å for each of the spheres and 3.9 Å for the radius of the cylinder).

As a preliminary check of the reliability of the model, we have computed its accessible volume using the probe–sphere algorithm.[47] A sphere of a given radius is rolled over the surface of the molecule of interest; the surface described by the center of the sphere in its journey limits the available and inaccessible volumes. Full atom B-DNA accessible volumes have been reported by Demaret and Guéron[48] using van der Waals radii for the atoms and a probe radius of 2.35 Å. The comparison between both models is difficult because the latter model is a hard body while the GP is not. The van der Waals radii used in the Demaret–Guéron calculations do not have a clear correspondence in our model. On the other hand, we are not interested in a detailed description of DNA but instead in a model with its essential features. So we have freely tried different probe radius. A size of 1.6 Å seems to furnish interesting results. These are presented in Fig. 2 along with the curve for the full-atom van der Waals model. The volumes are given in a derivative mode, i.e., the y axis is the derivative of the volume with respect to the radial distance. Thus, the total volume of the enclosed cylinder, namely, $2\pi rh$ with $h=33.8$ Å—a full DNA helix turn is used—is a straight line. The area below a curve at a given radial coordinate indicates the volume inaccessible to the ions, while the area between the line and the straight line gives the accessible volume.

Given the simplicity of the GP model, the agreement is remarkable not only because the total volumes are similar but rather because the similarity is observed at any value of the radial coordinate. This means that our model adequately represents the grooved surface of real DNA. It can be argued

Downloaded¬27¬May¬2005¬to¬147.96.5.17.¬Redistribution¬subject¬to¬AIP¬license¬or¬copyright,¬see¬http://jcp.aip.org/jcp/copyright.jsp

that our probe radius is somewhat small but we believe that there are other properties more relevant for a fine tuning of the model. For instance, Poisson–Boltzmann results[49] indicate that the hard spheres diameters equivalent to the soft spheres of the GP model are overestimated by about 0.5 Å, which would be equivalent to the use of a probe radius of 2.1 Å.

The GP model is computationally almost as inexpensive as any other model incorporating a discretely charged scheme such as the DS one. The only extra distances that must be computed in calculating the interaction of an ion with DNA are those to the intermediate spheres. As the interaction with these spheres is only repulsive, the use of a cutoff can be safely invoked, greatly diminishing the number of interactions of this kind.

III. THE SIMULATIONS

Monte Carlo simulations have been performed for the DNA models described above covering a broad range of bulk concentrations, from 0.01 to 2.5 M. The simulated states are given in Table I. They have been chosen to allow a systematic comparison between models. We will refer to the simulations by its nominal concentration, keeping in mind that the actual bulk salt concentration is that observed in the simulation far away from the polyelectrolyte (see below). As far as we are aware, results for systems up to 1 M have been previously reported for the homogeneously charged cylinder[36] and only up to 0.1 M for a grooved DNA.[45] Thus, the simulations presented in this work extend the previous concentration range to cover higher ones. This high salt regime is very interesting in many respects. In particular, the salt-induced transition from the B to the Z forms of DNA appears at about a 2.3 M NaCl concentration[50,51] (incidentally, strictly speaking, the simulations at a bulk concentration of 2.5 M correspond to a state in which the B-DNA form is in the minority).

A. Boundary conditions

Periodic boundary conditions are used in the axial direction giving the desired infinitely long polyion. The simulations below 0.25 M have been done with the cell model,[34] in which a (hard) cylindrical boundary limits the space available to the ions. The cell is placed far enough from the DNA to allow a complete relaxation of the ionic density profile, so that a defined bulk phase (i.e., equal concentration of coions and counterions) is obtained. The measured bulk concentrations are given in the last column of Table I. Thus, we implicitly assume an infinitely diluted DNA. This is different to what the cell model commonly implies, namely, the cell size dictates the polyion concentration.

More concentrated salt solutions are, on the other hand, significantly affected by the presence of the hard boundary[36] resulting in a spurious attractive potential.[52] For these systems, the modulated bulk as fuzzy boundary method[36] (MBFB), which proved its usefulness in the simulation of long-ranged inhomogeneous systems, has been used instead. In this method, the cylinder corresponding to the cell model (the inhomogeneous region) is immersed in a periodic box (a hexagonal prism in our case) filled with bulk solution and the hard wall removed, so that mobile ions are able to cross the boundary. The ions interact with the surrounding bulk through a discrete particle–particle modulated (short-ranged) Coulomb potential[53] while the missing tail is recovered as a mean field contribution computed in a self-consistent way. The simulation with the HS model at 1 M corresponds to the run labeled M^B in Ref. 36. In the other cases, the modulating radius have been chosen to include 10 ions on average.[36]

B. Axial long-range potential

It is well established that, in computer simulation of charged inhomogeneous systems, the interactions of each particle must include the part of the system along the directions for which periodic boundary conditions are used.[54] This is due to the fact that the anisotropic charge distribution is repeated *ad infinitum* in those directions.[36] We have employed the method pioneered by Torrie and Valleau for the case of the planar electrical double layer.[54] There, the effect of the charge distribution outside the simulation cell is included as a mean field term computed self-consistently from the average charge distribution within the cell. The appropriate formulas for the case of homogeneously charged polyions are given, for example, in Ref. 36. The simulations of the HH model have been performed with the SMFK program by Vorontsov-Velyaminov and Lyubartsev[39] available from the CCP5 program library which implements a version of the Ewald summation developed for systems that are periodic in one dimension. The simulation at 0.01 M concentration was repeated with the long-range potential via the mean field approach. The results were indistinguishable. To our knowledge, this is the first observation of the equivalence of these two long-range correction methods.

When the polyelectrolyte is made up of discrete charges, the long-range correction formulas used for the homogeneous models are no longer valid. The electrostatic field created by a discretely charged DNA model extended periodically along the axial direction can be obtained as that of a sum of arrays of discrete charges placed along lines parallel to the DNA axis. The potential between an ion i and an infinitely long array of discrete charges is

$$U_{i\nu}^{\text{array,inf}}(\rho_{i\nu},\Delta z_{i\nu}) = 2z_i\xi_\nu\beta^{-1}\left[\log(\rho_{i\nu}) - 2\sum_{j=1}^{\infty} K_0(\kappa_j\rho_{i\nu})\cos(\kappa_j\Delta z_{i\nu})\right], \tag{3.1}$$

where $\rho_{i\nu}$ is the distance from the ion to the array ν, ξ_ν the reduced axial charge density of the line, $\kappa_j = 2\pi j/b_\nu$ (b_ν being the distance between two consecutive charges along the array), $\Delta z_{i\nu}$ the axial coordinate of the ion with respect to the closest charged site of the array, and K_0 is the modified Bessel function of order zero and second kind. The above equation is obtained by expanding the point-charge potentials in cylindrical coordinates.[55] The first term is the potential of an infinite homogeneous line of charge and the second

Downloaded¬27¬May¬2005¬to¬147.96.5.17.¬Redistribution¬subject¬to¬AIP¬license¬or¬copyright,¬see¬http://jcp.aip.org/jcp/copyright.jsp

is the charge discreteness contribution. The total potential between the charges in an infinite DNA helix and a mobile ion is then

$$U_{\mathrm{ip}}^{\mathrm{sites},\infty}=\sum_{\nu} U_{i\nu}, \tag{3.2}$$

where the sum extends over the 20 arrays of charge (in the case of our models for B-DNA, there are 20 charged sites—10 phosphorus atoms in each of the strands—and thus $\xi_\nu=\xi/20$). The summation in the right-hand side of Eq. (3.1) is quickly convergent so few terms are needed. In this way, the equation can be more efficient than the explicit sum over each of the polyelectrolyte charged sites—Eq. (2.8)—for simulation cells made of three or more turns along the axial direction. But the main advantage of the above formulas lie in the fact that the long-range corrections are evaluated as accurately as needed. An alternative method was employed by Gordon and Goldman[23] who approximated the polyion segments outside the simulation cell by uniformly charged cylinders. This is an acceptable approximation if the axial length of the cell is quite long but it is not so for useful size cells.[56]

The long-range correction due to the potential created by the mobile ions outside the simulation cell has been calculated by using the radial density profile. The justification for this is that the ionic charge density profile in the axial direction is not as inhomogeneous as that of the polyelectrolyte because the charged sites of the latter are kept fixed while the ions are mobile and, thus, undergo thermal fluctuations which reduces the inhomogeneity. The equivalence between the Ewald summation and the mean field approach commented above furnishes further support for this approximation.

C. Other simulation details

In polyelectrolyte systems with added salt in the dilute regime, convergence problems of the Markov chain can occur.[57] These are due to the strong inhomogeneity of the counterions' distribution along the radial direction, changing from about one molar near DNA to the corresponding bulk concentration (which may be several orders of magnitude smaller). Jayaram and co-workers[21] resorted to multiple particle moves to improve convergence. To solve this problem, a density scaled sampling scheme was proposed by Gordon and Goldman.[57] In this method, the ion trial displacement parameter varies with the distance to the polyelectrolyte; it is small near it and large far away. The method furnishes reasonable acceptance rates (say in the range 0.3–0.6) at all distances. Of course, the acceptance algorithm must be modified accordingly.[57] We have used the density scaled sampling method in all cell model simulations but those for the hard homogeneously charged system. Efficient sampling and fast convergence were achieved. On the other hand, simulations with a modulated bulk as a fuzzy boundary employ classical Metropolis sampling as they refer to quite concentrated systems where the inhomogeneity across the box is small.

The simulations start by randomly placing the mobile ions within the simulation box but avoiding overlaps among them and the DNA. After a number of pre-equilibration cycles, the density profiles are computed so the long-range external potential can be evaluated. An equilibration period follows, in which the density profiles and the external potential attain self-consistency. In the MBFB simulations, the correction potentials are also evaluated in the self-consistency period.[36] About 20 000 cycles were used for the complete equilibration period (a cycle means as many single-particle moves as the number of mobile ions). Finally, the production phase begins. The number of cycles in this period ranged from 20 000 to 40 000.

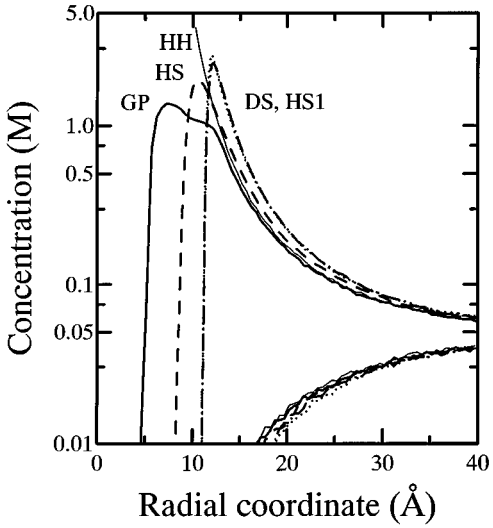

FIG. 3. Concentration profiles for different DNA models at 0.05 M bulk concentration. The top curves are for counterions and the bottom ones for coions. GP model (thick solid line), HS (dashed), DS (dotted), HS1 (dash-dotted), and HH (thin solid). Notice the logarithmic scale of the concentration axis.

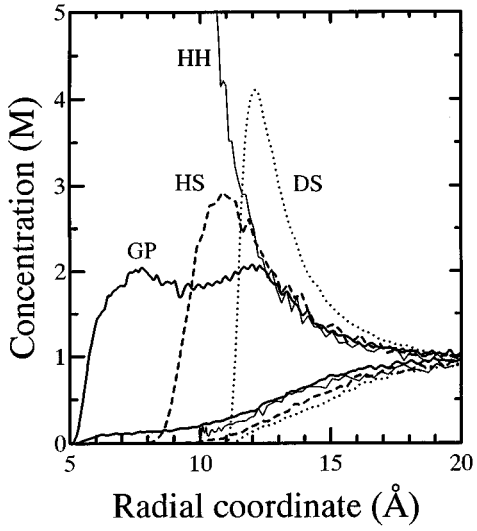

FIG. 4. Same as Fig. 3 but at 1 M bulk concentration.

Downloaded¬27¬May¬2005¬to¬147.96.5.17.¬Redistribution¬subject¬to¬AIP¬license¬or¬copyright,¬see¬http://jcp.aip.org/jcp/copyright.jsp

IV. RESULTS AND DISCUSSION

The radial density profiles for the simulations at 0.05 and 1 M supporting electrolytes are displayed in Figs. 3 and 4, respectively. Qualitatively, the figures are consistent with the known picture of the ionic atmosphere around highly charged cylindrical polyelectrolytes which has recently been confirmed by experimental measurements using small-angle neutron scattering.[58,59] A condensation of counterions occur close to the DNA surface resulting in a concentration in the molar range irrespective of bulk salt concentration; the energetic gain of this counterion distribution in the strong polyion electrostatic field compensates for the entropic cost to assemble it. Beyond this condensation region, the distribution falls to the bulk value in a Poisson–Boltzmann-type manner. The profiles go smoothly to zero as one approaches the DNA axis for the soft repulsive systems and give a nonzero contact value in the case of the hard model. The comparison between the homogeneously charged models shows that the soft repulsive cylinder (HS) gives quite similar results to that of the hard one (HH) suggesting some equivalence between those hard and soft models in a wide concentration range. Moreover, it is to be noticed that despite its simplicity the HH model closely matches the results of the (considerably more sophisticated) grooved model from about 12 Å.

For polyelectrolytes with soft repulsive potentials, the mobile ions are able to penetrate into the DNA and, thus, the maximum in the counterion density profile is lowered. This results in a similar number of condensed counterions at medium distances except in the case of the models with the origin of the repulsive potential displaced from the DNA axis (models DS and HS1). The density profiles at intermediate and large distances seem to indicate that those models are too repulsive. As the choice for the steepness parameter was intended to provide a soft potential in some way equivalent to a hard cylinder with the typically used distance of closest approach of 12 Å, we must agree with Jayaram *et al.*[28] in that such distance is too high. The acceptable coincidence in the concentration profiles of the GP, HS, and HH models for moderate to long distances indicates that a value of 10 Å seems more adequate (8 Å corresponding to the macromolecule and 2 Å to a mobile ion in contact). This value matches that suggested by recent small-angle neutron scattering studies on DNA salt-free systems[58,59] which estimate the DNA radius in 8 Å. The comparison between the results for the GP, HS, and HH at medium and large distances is difficult due to the statistical noise of the concentration profiles. Besides, a trivial analysis in terms of these functions sometimes masks significant differences. It has been shown in the context of simple electrolyte solutions that the charge compensation functions are at the same time much less noisy and a more stringent test for comparison.[38,41] Thus, a more thorough discussion is delayed until the charge neutralization results.

The most striking feature of the density profiles in Figs. 3 and 4 is the double humped structure of the GP model counterions curve. The first maximum at about 7.5 Å corresponds to counterions located inside the DNA grooves, while the second at 12 Å is due to the cations that condensate near the macromolecule by virtue of its charge density which, at this distance, is about half that of B-DNA (see below) due to partial compensation by counterions in the grooves. Both maxima are about the same height so that between 7 and 12 Å the concentration is roughly constant. In Fig. 5 the ratio of local to bulk concentration $C(\rho)/C_{\text{bulk}}$ is displayed for the GP model at the simulated states (the most concentrated system is not drawn for clarity). As the added salt concentration diminishes, the inner maximum gets slightly higher than the second but they remain always within the same order of magnitude. The stronger inhomogeneity of the more diluted solutions is apparent from their higher $C(\rho)/C_{\text{bulk}}$ ratios at all distances.

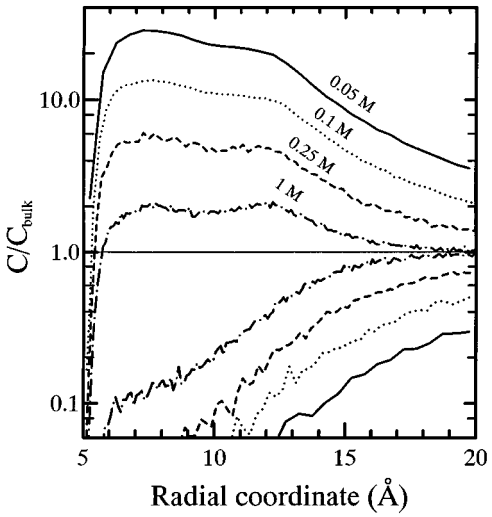

FIG. 5. Ratio of local to bulk concentration for the GP model at different bulk concentrations. Counterions curves are those exhibiting C/C_{bulk} values greater than 1 while the coions results are below the unity line. 0.05 M (solid line), 0.1 M (dotted line), 0.25 M (dashed line), and 1 M (dash-dotted line). Notice the logarithmic scale of the concentration ratio axis.

The double hump in the counterions' profile was already observed in the salt-free Brownian dynamic simulations of Guldbrand *et al.*[25] As they used a full atom representation of DNA and a more complex charge distribution, the ability of a relatively simple model as GP in predicting this structural feature is a pleasant result. A salt-free simulation with the GP model (using a finite cell boundary) at the conditions of Guldbrand's larger box (their simulation C4 corresponding to a 0.15 M phosphate concentration) gives peaks of similar height and at the same positions. A detailed comparison is out of place here (see the discussion below in the charge neutralization paragraphs) due to the differences in the ions size, repulsive potentials involved, and (specially) boundary conditions used. Nevertheless, the trends are completely similar to that observed in the comparison of the volumes between the GP model and the full atomic DNA (see Fig. 2). Furthermore, Guldbrand *et al.*[25] proved that the ions distribution of the continuum solvent model agrees with that of a simulation in which explicit water was included. Therefore, we may conclude that our simple GP model reproduces the behavior of full atomic DNA simulations with explicit water, at least with respect to cylindrically averaged ionic concentration profiles.

Downloaded¬27¬May¬2005¬to¬147.96.5.17.¬Redistribution¬subject¬to¬AIP¬license¬or¬copyright,¬see¬http://jcp.aip.org/jcp/copyright.jsp

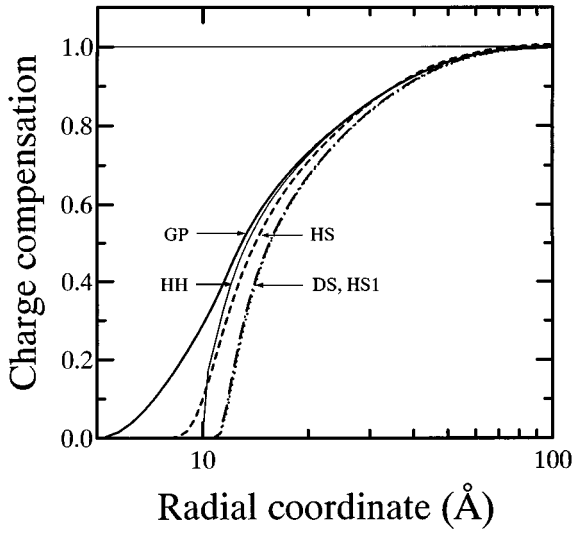

FIG. 6. Charge compensation function for different DNA models at 0.05 M bulk concentration. GP model (thick solid line), HS (dashed line), HS1 (dash-dotted line), DS (dotted line), and HH (thin solid line). The limiting value $Q(\infty)=1$ is shown as an horizontal line.

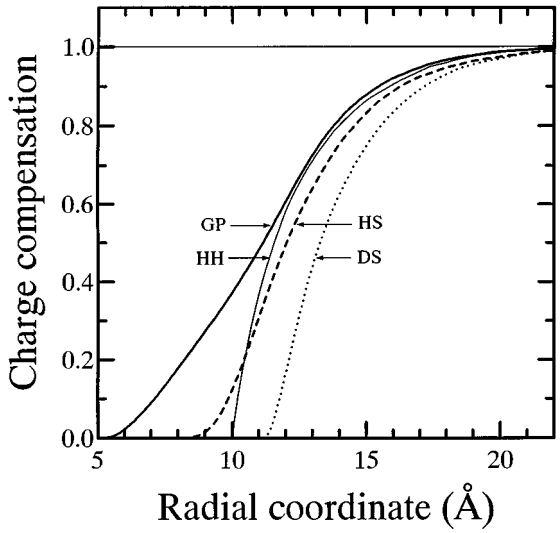

FIG. 7. Same as Fig. 6 but at 1 M bulk concentration.

With regard to coions (Fig. 4), although the differences among systems are now smaller, the penetrabilities are kept as for counterions. The main point to be stressed is the small but significant number of coions within the grooves of the GP model at 1 M bulk concentration (and above). Curiously, at this concentration, the HH model gives a nonzero coion density profile at the cylinder surface and the best coion overall agreement with the GP model among all the models.

The way in which the mobile ions gradually cancel the polyion charge is described by the charge compensation function $Q(\rho)$ given by

$$Q(\rho)=\sum_i q_i(\rho), \tag{4.1a}$$

$$q_i(\rho)=z_i\int_0^b\int_0^{2\pi}\int_0^{\rho}C_i(\rho')\rho' d\rho' d\phi dz, \tag{4.1b}$$

where the sum extends over ionic species. $Q(\rho)$ is zero at $\rho=0$ and increases with distance reaching the unity at the bulk. Besides, it gives the radius of the area of condensed ions in the counterion condensation theory[4–6]—the so-called Manning radius, R_M—via $q_+(R_M)=1-1/\xi$; for B-DNA $q_+(R_M)=0.76$. Notice that within the CC theory $Q(R_M)=q_+(R_M)$, as no coions are allowed within the condensation region. The neutralizing charge functions for all the models in dilute solutions and at concentrated conditions are shown in Figs. 6, 7, and 8 (0.05, 1, and 2.5 M, respectively), while the curve for the GP model with no added salt is compared with full-atom DNA results[25] in Fig. 9. In the first plot of the series (Fig. 6), the changes due to variations in the model can be appreciated. The penetration sequence manifests in a quicker cancellation of a fraction of the DNA charge. After that, all models exhibit a monotonous increase of the charge compensation. At distances close to the region for which the polyelectrolyte charge is almost completely canceled, all the curves converge in a Poisson–Boltzmann-type manner. The overall behavior observed at 0.05 M is kept at much higher concentrations. In fact, the same holds for DNA in a 1 M solution. As previously stated, the charge compensation functions are less noisy than the concentration profiles. Besides, the former manifest more clearly the departures between different systems. For instance, some attention is needed to realize that, beyond the statistical error, the counterion profile for the HS curve is slightly (but rather systematically) above that of the HH system at medium to large distances both at 0.05 and 1 M (Figs. 3 and 4). As the opposite holds for the coions curve, the charge compensation functions show departures between both systems which are somewhat larger than expected in a simple inspection of the concentration profile plots. Even with these comments in mind, the overall agreement between the results for both systems is quite satisfactory. In this context, it is remarkable that the simple HH model gives good results compared with the

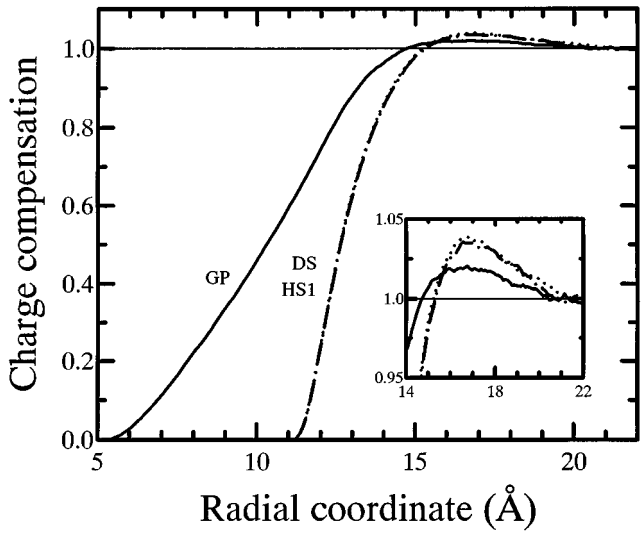

FIG. 8. Same as Fig. 6 but at 2.5 M bulk concentration. The inset shows an enlargement of the region in which the charge reversal takes place.

Downloaded¬27¬May¬2005¬to¬147.96.5.17.¬Redistribution¬subject¬to¬AIP¬license¬or¬copyright,¬see¬http://jcp.aip.org/jcp/copyright.jsp

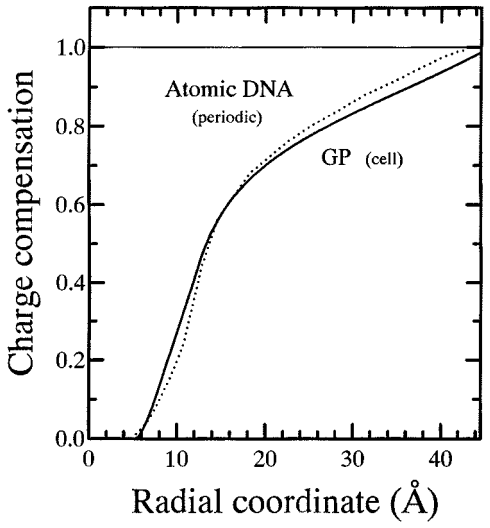

FIG. 9. Comparison of the charge compensation functions for full-atom DNA (dotted line) and the GP model (solid line) with no added salt.

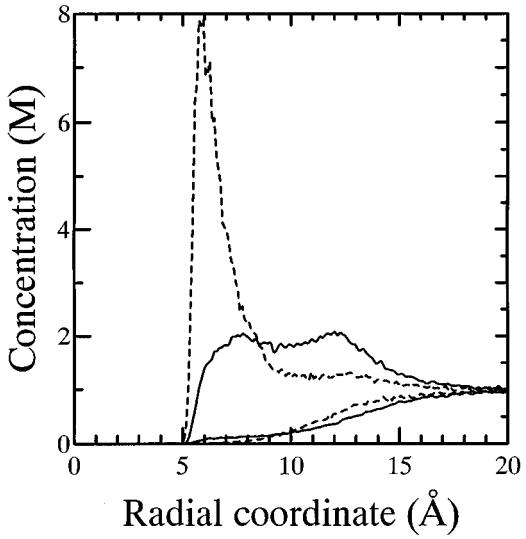

FIG. 10. Comparison of the concentration profile at 1 M bulk for the GP model (solid line) and the same model but with its charge homogeneously distributed along the axis (dashed line, see the text).

GP model from about 12 Å. This can be understood if one realizes that the counterions accommodated into the grooves of the GP model have the same effect as the dense sheet condensed into the hard surface of the HH model (see Fig. 4). We may thus talk of an equivalence in the long-range properties between hard and soft models when the hard core radius is appropriately chosen. Notice that the equivalence is kept in a wide concentration range for the same value of the hard diameter.

In Figs. 6 and 8 we have compared the charge compensation function for the DS model with that of a homogeneously charged one with exactly the same repulsive forces (the HS1 model) in presence of 0.05 and 2.5 M concentration of added salt, respectively. In both cases, the DS and HS1 curves are so close that they are barely discernible. It must be concluded that the introduction of discrete charges by itself does not modify the behavior of a simple model. However, discreteness effects are more important for low-charged systems ($\xi<1$)[16] so this assertion may not apply to other polyelectrolytes. When the charge discreteness is supplemented with an appropriate treatment of the excluded volume (our GP model, for example) the results are substantially different. An analogous statement holds for the excluded volume: the details in the polyelectrolyte shape are important only if the charges are placed in positions at which a substantial coupling between coulombic and repulsive (packing) forces can occur. In fact, only to confirm this point we carried out a simulation of a model with the same shape as the grooved model but homogeneously charged along the DNA axis. The density profile for this model is compared with the original GP model at 1 M bulk concentration in Fig. 10. The system behaves like the plain homogeneously charged model with the counterions condensed around the internal cylinder, the typical effect of the intermediate and phosphate spheres (the double hump in the counterion concentration profile) being almost completely blurred.

Leaving aside the comments in the previous paragraph, at the higher concentration, there are very important changes with respect to the behavior at 1 M concentration. In systems with 2.5 M added salt, an interesting phenomenon arises. From about 15 Å, the ionic cloud not only compensates for all the polyelectrolyte charge but even *exceeds it*. The appearance of charge fluctuations is a novel result for DNA but not for other polyelectrolyte systems. In fact, it has already been observed in electrophoresis experiments with other strong polyelectrolytes;[60] there, a cationic polyion was found to migrate towards the anode at certain concentrations of added 1:1 salt. The same behavior is exhibited by 2:2 electrolytes in the vicinity of a polyelectrolyte as shown both by MC simulations[14] and the HNC integral equation.[61] The HNC also predicts overneutralization for a soft polyion and a 2:1 salt.[62] Finally, monovalent electrolytes give charge inversion in the context of the planar electrical double layer.[63] The importance of our observation lies in the fact that the simulation results give the ''exact'' properties of the models and it is then free from theoretical approximations. It is our belief that the the charge reversal has not been observed in DNA systems due to the high salt concentration required, not addressed in previous work. As seen in Fig. 8, not only a simple soft polyelectrolyte manifests charge overneutralization but so does the more realistic GP model, though less pronounced in the latter case. The role of ion–ion correlations for the occurrence of this phenomenon is categorically evidenced by the fact that the Poisson–Boltzmann equation, which neglects such correlations, never gives charge inversion irrespective of the charge and concentration of the added salt.[14,49]

We have delayed up to now an explicit comparison of the GP results with that for a full-atomic DNA.[25] The reasons for this have been commented on above but can be more easily understood with the help of Fig. 9 where the charge neutralization functions are displayed. The shape of both curves is similar and the overall agreement is highly satisfactory. Nevertheless, it should be stressed that the departures at long distances are quite significant since we must

Downloaded¬27¬May¬2005¬to¬147.96.5.17.¬Redistribution¬subject¬to¬AIP¬license¬or¬copyright,¬see¬http://jcp.aip.org/jcp/copyright.jsp

expect the same asymptotic behavior. It is simple to explain such significant differences as a consequence of the different boundary conditions used. The full atomic simulations corresponded to an ordered (hexagonally packed) DNA solution, which implies that the slope of the curve at large distances from the polyelectrolyte should decrease reaching a zero value in the zone between two neighboring DNA, whereas our study gives a nonzero slope due to the absence of polyions beyond the cell boundary. This may be seen in Fig. 4 of Jayaram *et al.*[21] where the full-atom DNA was also considered, although we prefer to compare with Guldbrand results because in Jayaram *et al.*'s simulations the long-range potential was included in an approximate way. Besides, the effect of neighboring DNA is added by virtue of the hexagonal boundary conditions, which results in more counterions near the box limits with respect to the cell model, as previously noticed by Groot.[64] Thus, the excess charge accumulated (or noncompensated) in the outer region must be compensated for in the vicinity of the polyelectrolyte. In view of the general agreement between both systems, this effect is likely to be responsible for most of the departures observed.

V. CONCLUSIONS

Monte Carlo simulation has been used to evaluate several properties of simple DNA models which essentially depend on the radial (cylindrically averaged) concentration profiles. The analysis of properties depending on the axial anisotropy (for the discretely charged models) is left for a forthcoming paper. As far as we are aware, these are the first simulations of discretely charged models using an exact formula to include the long-range correction due to the replicas of the simulation box along the axial direction. We have tried to compare the simulated results against available pseudoexperimental data. It is worth noting that a precise assessment of the models cannot completely be established. Due to the extreme complexity of the systems involved, the comparison with other simulation results (or accessible volume computations) is disturbed by the differences in the force fields employed, the degree of definition of the model or the boundary conditions used in the simulations. But despite the difficulties mentioned some conclusions can be safely established.

The first conclusion of this work concerns the equivalence between hard and soft models. Indeed, although this a general behavior in the liquid state it must be recalled here that an equivalent hard model exists for a given soft body so the latter models add very little as long as the properties calculated in this work are involved. It is to be stressed that despite its simplicity the hard homogeneously charged model (HH) closely matches the results of the (considerably more sophisticated) grooved model from about 12 Å. This means that the properties depending essentially on the number of condensed counterions can be accurately obtained with such an extremely simple model. In contrast, the counterions have no access to the innermost region. Thus, the structure in the zone close to the DNA axis is completely ignored. Soft models are able to predict some penetrability of the counterions but not in the degree manifested by the grooved model which reveals a more significant organization. The discretization of the charge of the polyion leads to similar conclusions. In fact, the dependence on the radial distance to the polyelectrolyte at which the repulsive forces are originated is far more important than the intrinsic effect due to the charge discreteness. The choice of the origin of repulsive forces can mask the comparisons so some care is needed. When this is done (the pairs of models HH/HS and DS/HS1), a global equivalence between homogeneously and discretely charged models is observed. (Incidentally, the comparison of the results for these pairs of models with the more sophisticated grooved one, seems to indicate that the effective distance of closest approach polyelectrolyte–counterion is about 10 Å—instead of the usual value 12 Å—corresponding to an effective DNA radius of about 8 Å, a value supported by recent studies of small-angle neutron scattering experiments.)[58,59] We must conclude that the inclusion of soft potentials and/or discrete charges do not modify essentially the predictions of the HH model.

In contrast, the incorporation of the grooved nature of DNA into a discretely charged model has interesting structural implications. It seems that the coupling between excluded volume effects together with a discrete charge distribution at the polyion brings about new structural features, the more important of them being the splitting of the first peak of the counterion concentration profile which is resolved in a double hump already observed in a full atomic DNA simulation. Our simple grooved scheme is able to predict this important feature. Other properties that compare favorably with pseudoexperimental data are the accessible volume and charge compensation. In summary, our ''grooved primitive'' is a model intermediate between the extreme simplicity of the hard homogeneously charged system and the complexity of a full atom DNA description but whose properties are very close to the latter one.

The effect of the added salt is gradual for concentrations up to 1 M. Compared with this behavior, there is a dramatic change when the concentration is increased to 2.5 M. In these systems, the ionic cloud around DNA not only compensates for its full charge but even exceeds it, giving rise to a charge reversal phenomenon. This feature is present in all models studied, independent of its repulsive potential or charge description. It seems that this is the first observation of the phenomenon probably due to the high salt concentration required to detect it. Finally, it is worth noting that the concentration range at which the overneutralization appears is coincident with that at which the salt induced B→Z-DNA transition takes place.[50,51] Investigations along these lines will be reported in forthcoming papers.

ACKNOWLEDGMENTS

This work was partially supported by Grant No. PB93-0085 furnished by the Dirección General de Investigación Científica y Technológica of Spain. J.C.G.M. acknowledges a FPI grant from the Spanish Ministry of Education, and is very grateful to Dr. H. L. Gordon for helpful correspondence.

Downloaded¬27¬May¬2005¬to¬147.96.5.17.¬Redistribution¬subject¬to¬AIP¬license¬or¬copyright,¬see¬http://jcp.aip.org/jcp/copyright.jsp

[1] J. O'M. Bockris and A. K. N. Reddy, *Modern Electrochemistry* (Plenum, New York, 1970).
[2] W. Saenger, *Principles of Nucleic Acid Structure* (Springer, New York, 1984).
[3] A. Katchalsky, Pure. Appl. Chem. **26**, 327 (1971).
[4] G. S. Manning, J. Chem. Phys. **51**, 924 (1969).
[5] G. S. Manning, J. Chem. Phys. **51**, 934 (1969).
[6] G. S. Manning, J. Chem. Phys. **51**, 3249 (1969).
[7] G. S. Manning, Phys. Chem. **7**, 95 (1977).
[8] T. L. Hill, Arch. Biochem. Biophys. **57**, 229 (1955).
[9] R. A. Marcus, J. Chem. Phys. **23**, 1057 (1955).
[10] P. Mills, C. F. Anderson, and M. T. Record, Jr., J. Phys. Chem. **89**, 3984 (1985).
[11] C. F. Anderson and M. T. Record, Jr., Annu. Rev. Phys. Chem. **33**, 191 (1982).
[12] C. S. Murthy, R. Bacquet, and P. J. Rossky, J. Phys. Chem. **89**, 701 (1985).
[13] P. Mills, M. D. Paulsen, C. F. Anderson, and M. T. Record, Jr., Chem. Phys. Lett. **129**, 155 (1986).
[14] V. Vlachy and A. D. J. Haymet, J. Chem. Phys. **84**, 5874 (1986).
[15] M. D. Paulsen, B. Richey, C. F. Anderson, and M. T. Record, Jr., Chem. Phys. Lett. **139**, 448 (1987).
[16] D. Soumpasis, J. Chem. Phys. **69**, 3190 (1978).
[17] L. Guldbrand, Mol. Phys. **67**, 217 (1989).
[18] D. L. Beveridge and G. Ravishanker, Current Opinion Struct. Biol. **4**, 246 (1994).
[19] B. Jayaram, N. Aneja, E. Rajasekaran, V. Arora, A. Das, V. Ranganathan, and V. Gupta, J. Sci. Indust. Res. **53**, 88 (1994).
[20] K. J. McConnell, R. Nirmala, M. A. Young, G. Ravishanker, and D. L. Beveridge, Biophys. J. **66**, 391 (1994).
[21] B. Jayaram, S. Swaminathan, D. L. Beveridge, K. Sharp, and B. Honig, Macromolecules **23**, 3156 (1990).
[22] P. E. Smith and W. F. van Gusteren, J. Mol. Biol. **236**, 629 (1994).
[23] H. L. Gordon and S. Goldman, J. Phys. Chem. **96**, 1921 (1992).
[24] F. Gago and W. G. Richards, Mol. Pharmacol. **37**, 341 (1990).
[25] L. E. Guldbrand, T. R. Forester, and R. M. Lynden-Bell, Mol. Phys. **67**, 473 (1989).
[26] C. Tanford and J. G. Kirkwood, J. Am. Chem. Soc. **79**, 5348 (1957).
[27] M. Troll, D. Roitman, J. Conrad, and B. H. Zimm, Macromolecules **19**, 1186 (1986).
[28] B. Jayaram, K. A. Sharp, and B. Honig, Biopolymers **28**, 975 (1989).
[29] J. Conrad, M. Troll, and B. H. Zimm, Biopolymers **27**, 1711 (1988).
[30] G. R. Pack, G. A. Garrert, L. Wong, and G. Lamm, Biophys. J. **65**, 1363 (1993).
[31] B. E. Hingerty, R. H. Ritchie, T. L. Ferrel, and J. E. Turner, Biopolymers **24**, 427 (1985).
[32] B. Halle and L. Piculell, J. Chem. Soc. Faraday Trans. 1 **78**, 255 (1982).
[33] J. C. Leyte, Makromol. Chem. Macromol. Symp. **34**, 81 (1990).
[34] R. M. Fuoss, A. Katchalsky and S. Lifson, Proc. Natl. Acad. Sci. USA **37**, 579 (1951).
[35] T. G. Wensel, C. F. Meares, V. Vlachy, and J. B. Matthew, Proc. Natl. Acad. Sci. USA **83**, 3267 (1986).
[36] J. C. Gil Montoro and J. L. F. Abascal, Mol. Simul. (in press).
[37] P. J. Rossky, J. B. Dudowick, B. L. Tembe, and H. L. Friedman, J. Chem. Phys. **73**, 3372 (1980).
[38] J. L. F. Abascal and P. Turq, Chem. Phys. **153**, 79 (1991).
[39] P. N. Vorontsov-Velyaminov and A. P. Lyubartsev, Mol. Simul. **9**, 285 (1992).
[40] F. Bresme and J. L. F. Abascal, J. Chem. Phys. **99**, 9037 (1993).
[41] J. L. F. Abascal, F. Bresme, and P. Turq, Mol. Phys. **81**, 143 (1994).
[42] J. C. Gil Montoro, F. Bresme, and J. L. F. Abascal, J. Chem. Phys. **101**, 10 892 (1994).
[43] D. M. York, T. Darden, D. Deerfield II, and L. G. Pedersen, Int. J. Quantum Chem. Quantum Biol. Symp. **19**, 145 (1992).
[44] S. Arnott and D. W. Hukins, Biochem. Biophys. Res. Commun. **47**, 1504 (1972).
[45] B. Jayaram and D. L. Beveridge, J. Phys. Chem. **95**, 2506 (1991).
[46] A. Rey and J. Skolnick, J. Chem. Phys. **100**, 2267 (1994).
[47] M. L. Connolly, Science **221**, 709 (1983).
[48] J. P. Demaret and M. Guéron, Biophys. J. **65**, 1700 (1993).
[49] J. C. Gil Montoro and J. L. F. Abascal (unpublished).
[50] F. M. Pohl and T. M. Jovin, J. Mol. Biol. **67**, 375 (1972).
[51] D. M. Soumpasis, Proc. Natl. Acad. Sci. USA **81**, 5116 (1984).
[52] A. Brunger, C. L. Brooks, and M. Karplus, Chem. Phys. Lett. **105**, 495 (1984).
[53] C. L. Brooks, B. M. Pettitt, and M. Karplus, J. Chem. Phys. **83**, 5897 (1985).
[54] G. M. Torrie and J. P. Valleau, J. Chem. Phys. **73**, 5807 (1980).
[55] J. D. Jackson, *Classical Electrodynamics* (Wiley, New York, 1967).
[56] J. C. Gil Montoro and J. L. F. Abascal (to be published).
[57] H. L. Gordon and S. Goldman, Mol. Simul. **3**, 213 (1989).
[58] J. R. C. van der Maarel, L. C. A. Groot, M. Manderl, W. Jesse, G. Jannink, and V. J. Rodriguez, J. Phys. II (France) **2**, 109 (1992).
[59] L. C. A. Groot, M. E. Kuil, J. C. Leyte, J. R. C. van der Maarel, J. P. Cotton, and G. Jannink, J. Phys. Chem. **98**, 10 167 (1994).
[60] U. P. Strauss, N. L. Gershfeld, and H. Spiera, J. Am. Chem. Soc. **76**, 5909 (1954).
[61] E. Gonzales-Tovar, M. Lozada-Cassou, and D. Henderson, J. Chem. Phys. **83**, 361 (1985).
[62] R. J. Bacquet and P. J. Rossky, J. Phys. Chem. **92**, 3604 (1988).
[63] L. Zhang, H. T. Davis, and H. S. White, J. Chem. Phys. **98**, 5793 (1993).
[64] R. D. Groot, J. Chem. Phys. **95**, 9191 (1991).

Downloaded¬27¬May¬2005¬to¬147.96.5.17.¬Redistribution¬subject¬to¬AIP¬license¬or¬copyright,¬see¬http://jcp.aip.org/jcp/copyright.jsp